Cellular and Molecular Biology

Journal homepage: www.cellmolbiol.org

Analysis of Inhibitory Effect of the Double-layer Nano-infusion on Vascular Restenosis in Animal Models of Coronary Atherosclerosis

Ge Cao, Hui Kang, Hui Yu, Qing He*

Department of Cardiovascular Surgery, West China Hospital of Sichuan University, Chengdu, 610041, Sichuan, China

ARTICLE INFO

Original paper

Article history:
Received: November 14, 2021
Accepted: March 11, 2022
Published: March 31, 2022

Keywords:
double-layer nanoparticle, paclitaxel, vascular endothelial growth factor, coronary atherosclerosis, restenosis, mouse model

ABSTRACT

This study aimed to investigate the effect of double-layer nano-infusion on restenosis in animal models of coronary atherosclerosis (CAD). For this purpose, forty Apolipoprotein E (APOE) gene mice ($ApoE^{-/-}$) were fed with 1.25% cholesterol, 10% fat, and 88.75% standard diet to establish CAD models. They were classified into the control group with paclitaxel nanoparticles (PTX-NPs) and the observation group with balloon infusion of PTX combined with vascular endothelial growth factor (VEGF) double-layer nanoparticles (V-P-NPs). The vascular endothelial healing and the occurrence of vascular restenosis were assessed. Results showed no significant differences in the particle size, distribution, and Zeta-potential between PTX-NPs and V-P-NPs (P>0.05). According to the transmission electron microscope (TEM), the nanoparticles had good dispersity, and the structure of the inner and outer layers of V-P-NPs was obvious. There were insignificant differences between the entrapment efficiency of PTX in PTX-PNS and the PTX and VEGF in V-P-NPs (94.32%, 95.66%, 97.89%) and drug-loading rate (28.91%, 30.12%, 29.91%) (P>0.05). The vascular endothelial healing degree of the observation group was better than that of the control group under optical coherence tomography (OCT). The restenosis, including the stenosis (6.91±7.59)%, proliferation (0.12±0.02), and the maximum intima thickness (0.07±0.09)mm of the observation group was decreased compared with the control group ((24.01±12.78)%, (0.28±0.01), (0.19±0.08)mm) (P<0.05). Then the double-layer nano-infusion therapy was conducive to healing vascular endothelial tissue and could effectively inhibit vascular restenosis, with clinical adoption value.

DOI: http://dx.doi.org/10.14715/cmb/2022.68.3.34

Introduction

As a common clinical disease, cardiovascular disease has high morbidity, disability, and even mortality, which brings serious effects on people's daily life. Coronary atherosclerotic heart disease (CAD) is one of them (1, 2). CAD is chronic heart disease. It is mainly caused by insufficient coronary blood supply due to atherosclerotic stenosis, which leads to heart ischemia and hypoxia (3). Currently, the main clinical treatment methods for CAD are percutaneous transluminal coronary angioplasty (PTCA) and scaffold implantation (4, 5). However, according to the statistical results of clinical treatment, restenosis occurs in many CAD patients after PTCA or scaffold implantation, which has aroused people's concern (6). Through the analyses, it has been proposed that vascular restenosis is closely related to the metastasis of vascular smooth muscle cells (VSMC) to intima (7). Further research is needed to effectively prevent the proliferation of VSMC.

Paclitaxel (PTX) is an anti-proliferation drug that has been adopted for the treatment of cardiovascular diseases for a long time, which can not only inhibit the proliferation of VSMC but also prevent restenosis (8, 9). Nonetheless, PTX can also inhibit the recovery of vascular endothelial injury due to certain damage to the endothelium of blood vessels during surgical treatment (10). As a growth and proliferation factor of endothelial cells (EC), vascular endothelial growth factor (VEGF) helps directly control the growth of EC, relieve vascular endothelial injury, and promote the repair of vascular endothelial (11). VEGF can promote the survival of EC by inhibiting the proliferation of VSMC, thus preventing thrombosis and inflammation (12). Consequently, VEGF combined with PTX has a certain preventive effect on vascular restenosis after the surgery of CAD. However, VEGF expression is mainly controlled by small interfering RNA (siRNA) molecules (13). Due to the hydrophilicity of siRNA, it isn't easy to be

*Corresponding author. E-mail: fengchizhi63@163.com

absorbed by cells, with a short half-life period, which affects the role of VEGF (14). Therefore, these problems need to be solved by improving the drug delivery systems.

The double-layer nanoparticle is a vital drug delivery system that is being explored at present (15). The double-layer nanoparticle is classified into the shell and content according to the different substances of the nano-carrier. Then, different therapeutic drugs are put into the inner and outer layers of double-layer nanoparticles to facilitate the multi-step release of drugs. Presently, double-layer nanoparticles have been applied in anti-breast cancer research, which has achieved good results (16). Moreover, double-layer nanoparticles are adopted for the cardiovascular scaffold coating to prevent restenosis, but the scaffold implantation is limited by the location of the lesion. To comprehensively explore the prevention of restenosis in CAD patients with double-layer nanoparticles administration, balloon infusion is adopted for administration. A drug balloon is a new technology that can distribute drugs evenly distributed on the blood vessel wall. It has a good adoption effect on the stenosis of blood vessels, with the wide recognition of people (17).

The animal model of CAD was established, which was treated with double-layer nano-infusion. The changes in atherosclerosis and the restenosis after local injection in vivo were assessed. It was hoped to provide an effective and feasible clinical treatment for patients with restenosis after the surgery of CAD.

Materials and methods

Model establishment and grouping

The Apolipoprotein E gene knockout mice (ApoE $^{-/-}$), a CAD animal model widely recognized by the international academic community, were selected as the research objects. Forty ApoE $^{-/-}$ mice (ApoEKO; B6.129 P2-ApoE tm1Unc, Jackson Laboratory, Bar Harbor, USA) were fed a standard diet of 1.25% cholesterol, 10% fat, and 88.75% to establish the CAD model. The mice were 12 months old, male, and weighed 480-500g. During the model establishment, the forty mice drank freely. The CAD model mice were averagely classified into the control group and observation group. Mice in both groups were treated with balloon infusion of nano drugs. The control group was only infused with PTX nanoparticles, and the observation group was treated with balloon infusion of PTX combined with the double-layer nanoparticles of VEGF. The adoption value of these two treatment methods was compared by evaluating the vascular endothelial healing and the occurrence of vascular restenosis in the two groups. The differences in age, gender, and weight weren't considerable between the two groups (P>0.05), and the experiment was feasible. Besides, this experiment was approved by the relevant veterinary medical committee.

Preparation of double-layer nanoparticles

To prepare the double-layer nanoparticle loaded with VEGF in the shell and PTX in the kernel (V-P-NPS), the first step was to prepare the PXT-loaded nanoparticles (PXT-NPs). The specific methods were as follows.

Firstly, 30mg of PXT (provided by Nanjing Zelang Biotechnology Co., LTD.) and 100g of polylactic-co-glycolic acid (PLGA) copolymer (provided by Sigma-Aldrich LLC., USA) were weighed and dissolved in dichloromethane. An ultrasonic probe crusher (CV26, Sonics & Materials, Inc., USA) was adopted to disturb the fused liquid at 30% power for 5 minutes every 40s and stop for 10s, during which 20mL 1% polyvinyl alcohol (PVA) was dropped into the fused liquid. The ultrasonic interference was followed for 10min (under an ice bath). The obtained liquid was then stirred at room temperature to volatilize methylene chloride. Subsequently, after it was centrifuged at 23,000rpm for 30min, it was washed with distilled water and centrifuged 3 times. Finally, the nanoparticles were suspended in 2mL distilled water, and they were dried and frozen (-80℃) for 24h to obtain PTX-NPs.

As for the preparation of V-P-NPs, 3g of VEGF plasmid (donated by Beijing Hospital) and the PXT-NPs obtained from the above steps were dissolved in 500μL distilled water and dropped into 2mL dichloromethane solution (ice bath containing 50mg PLGA). Colostrum was obtained by mixing at a speed of 20,000rpm for 5min with a high-speed mixer (purchased from IKA, Germany). Then, the colostrum was dropped to 15ml 1% PVA (under ice bath), with a stir in 3 gears of blender for 20min, and the multiple emulsion could be obtained. It was stirred for 3h under the greenhouse to make dichloromethane volatile. The over-speed centrifuge was employed at 23,000rpm for 30 min, and it was washed with

distilled water and centrifuged 3 times. Finally, the nanoparticles were suspended in 2mL distilled water and dried and frozen (-80℃) for 24h to obtain V-P-NPs.

Characterization of nanoparticles

Firstly, the nanoparticle size analyzer (Malvern Co., Ltd., Britain) was adopted to measure particle size, particle size distribution, and Zeta-potential through the principle of dynamic light scattering. All nanoparticles were detected 3 times to take the average, and the result was X+SD.

Secondly, transmission electron microscopy (TEM) was adopted to observe the morphology of nanoparticles, including form and size. The specific steps were as follows.

1mg of nanoparticle powder was weighed and dissolved in 1mL distilled water. A drop of the obtained V-P-NPS solution was placed on a copper mesh, which was air-dried overnight at room temperature. Then, the TEM was employed for observation.

Thirdly, the drug-loading rate and entrapment efficiency of nanoparticles were determined by high-performance liquid chromatography (HPLC). The specific approach was as follows.

The 5mg nanoparticles were dissolved in 1mL dichloromethane, and the dichloromethane was volatilized by ventilation. The free PTX and VEGF were dissolved in 1mL acetonitrile and filtered. Then, the 20μL sample was injected into a reverse C18 column (150x4.6 mm, 5μm) with an acetonitrile-water ratio of 1:1 at a flow rate of 1mL/min. The ultraviolet absorption of λ=227nm was detected 3 times as above, the average value was taken, and the result was X+SD. Equations (1) and (2) showed the calculation of drug-loading rate(Z) and entrapment efficiency(B), respectively.

$$Z = \frac{NPs_{(\mathrm{Drugs})}}{\Delta NPs} \times 100\% \quad [1]$$

$$B = \frac{\overline{\overline{NPs}}_{(\mathrm{Drugs})}}{NPs} \times 100\% \quad [2]$$

In Equations [1] and [2], $NPs_{(\mathrm{Drugs})}$ represented the amount of drug in nanoparticles, ΔNPs represented the total number of nanoparticles, $\overline{\overline{NPs}}_{(\mathrm{Drugs})}$ represented the measured drug content in nanoparticles, and NPs represented the theoretical drug content in nanoparticles.

Balloon medication method

All mice were anesthetized with 3% pentobarbital sodium, whose injuries were all induced by the same balloon. Electrocardiograph (ECG) monitoring was performed. The balloon was introduced into the femoral artery (the size of the balloon was chosen based on the outer diameter of the abdominal aorta), and the nanoparticles were injected at a dose of 1mg/kg. The control group was infused with PXT-NPs, and the observation group was infused with V-P-NPs. The nanoparticles were delivered through a GENIE catheter to the site of injury. Then, the catheter was removed after a 2-3 arm pressure was given for more than 5 minutes, and the proximal end of the femoral artery was ligated. The mice were fed aspirin (100 mg/day) and clopidogrel hydrogen sulfate (50 mg/day) for three consecutive days after surgery. After 4 weeks of a normal cholesterol diet, the endothelial cells and restenosis were observed.

Vascular endothelial healing

After 4 weeks of normal feeding, the endothelial tissues of mice were observed by optical coherence tomography (OCT). The imaging wire was located at the distal end of the OCT catheter. The OCT was placed on a conventional conductance wire and then moved from the distal end of the vessel to the proximal end at a speed of 1.5mm/s for morphological analysis. When the OCT was completed, the mice were euthanized, and arterial samples were obtained (fixed with 10% formalin) that were stained with hematoxylin-eosin (H&E). The histological analysis was performed with an optical microscope (OM).

Restenosis analysis

Postoperative target vessel stenosis was measured by quantitative coronary angiography (QCA), including the number of stenosis vessels, endothelial cell proliferation index, and maximum intima thickness. The artery was injected with normal saline. After it was frozen with liquid nitrogen, it was cut into 5μm segments and stained with H&E. OM was adopted to observe the lumen area and the new intima area, both of which were measured by the computerized surface survey.

Statistical methods

SPSS22.2 was employed for statistical processing. The measurement data were expressed as mean ± standard deviation. All data followed a normal distribution, and the *t*-test was adopted. Percentage (%) was how count data were represented, and the data were tested by χ^2 test. The difference was statistically considerable, with $P<0.05$.

Results and discussion

Particle size, distribution, and potential of nanoparticles

Figure 1 shows the detection results of particle size, distribution, and Zeta-potential of PTX-PNs and V-P-NPs. The particle size of PTX-PNS was (270.29±1.89) nm, the particle size dispersion coefficient was 0.152±0.02, and the mean value of Zeta-potential was (-4.11±0.29) mV. The particle size, distribution, and Zeta-potential of V-P-NPs were (251.12±1.19) nm, 0.155±0.02, and (-7.11±0.11) mV, respectively. The particle sizes of PTX-PNS and V-P-NPS ranged from 120nm to 300nm, which conformed to the permeability standard of the vascular inner layer, so it could be applied to research. Moreover, the difference wasn't considerable between the particle size distributions and Zeta-potential.

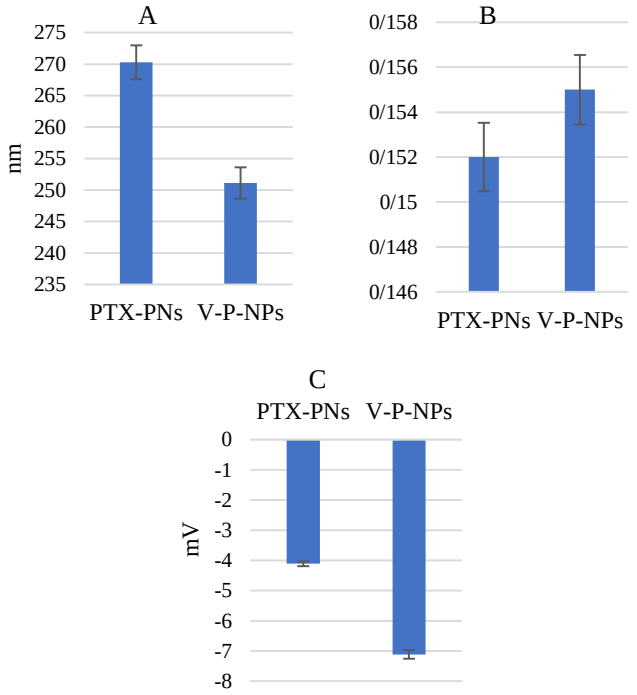

Figure 1. Particle size distribution and Zeta potential analysis of nanoparticles.

The characterization of nanoparticles

Figure 2 shows the morphology and size of PTX-PNs and V-P-NPs under TEM. The dispersity of PTX-NPs and V-P-NPs were all fine, both of which showed the spheroidal particles. The right image of Figure 2 shows the TEM observation result of V-P-NPs, from which the shell and inner layer structure of the double-layer nanoparticle could be observed. It indicated that the preparation of the double-layer nanoparticle of V-P-NPs was successful.

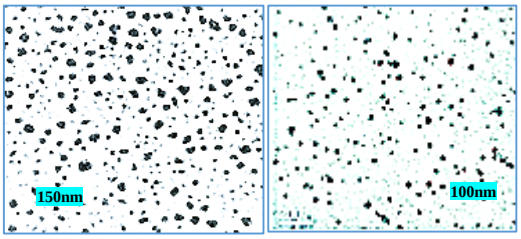

Figure 2. The results of TEM. (The left showed the results of PTX-NPs, and the right showed those of V-P-NPs).

Drug-loading rate and entrapment efficiency

Figure 3 shows the entrapment efficiency calculation results of PTX in PTX-PNs and PTX and VEGF in V-P-NPs. The entrapment efficiency of PTX in PTX-PNs was 94.32%, and that of PTX and VEGF in V-P-NPs were 95.66% and 97.89%, respectively. Therefore, the entrapment efficiency of effective drugs in PTX-PNs and V-P-NPs was very high. Figure 4 showed the drug-loading rate results of PTX in PTX-PNs and PTX and VEGF in V-P-NPs that were calculated by weight ratio. The drug-loading rate of PTX in PTX-PNs was 28.91%, and that of PTX and VEGF in V-P-NPs was 30.12% and 29.91%, respectively. The results showed that there was an insignificant difference in drug amount between the two nanoparticles ($P>0.05$).

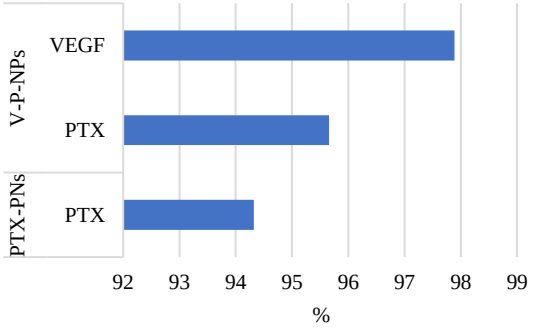

Figure 3. The results of entrapment efficiency.

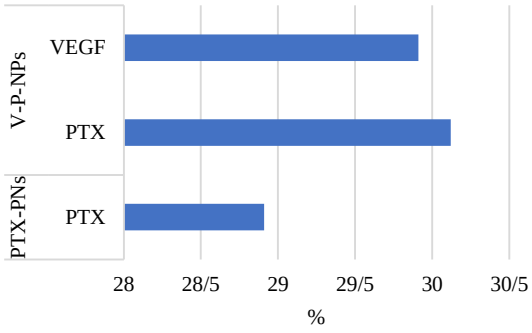

Figure 4. The results of the drug-loading rate.

Vascular endothelial healing

Figure 5 showed the healing of vascular endothelium in the two groups of mice under OCT. Figure 5A showed the normal OCT examination results of the vascular endothelium, and Figure 5B showed the vascular endothelium of mice in the control group. Through the comparison, the endothelial healing and proliferation of VSMC were inhibited in the control group. Figure 5C showed the changes in vascular endothelial of mice in the observation group, and the degree of complete endothelial healing was markedly better than that in the control group. Figure 6 showed the histological observation results of the vascular endothelium in mice under the corresponding OM, which reflected that the examination results were consistent with OCT results.

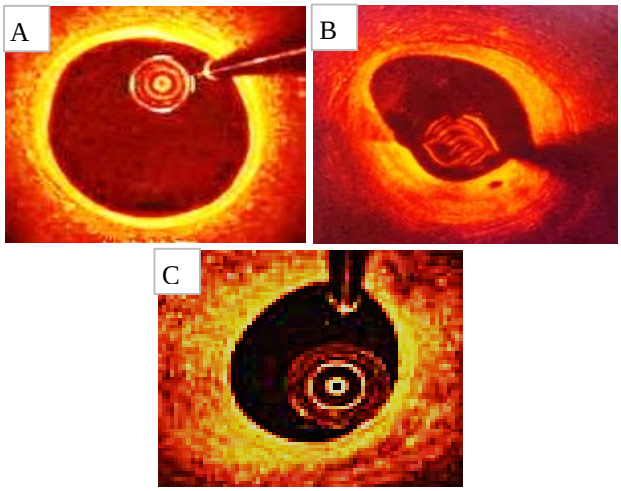

Figure 5. The results of the OCT examination.

Comparison of restenosis results

QCA was adopted to detect the number of narrow blood vessels, endothelial cell proliferation index, and maximum intima thickness of the mice in the two groups (Figure 7). In the control group, the stenosis of coronary arteries and vessels was (24.01±12.78) %, the proliferation index was (0.28±0.01), and the intima thickness was (0.19±0.08) mm. In the observation group, the stenosis of coronary arteries and vessels was (6.91±7.59) %, the proliferation index was (0.12±0.02), and the intima thickness was (0.07±0.09) mm. According to the comparison, the restenosis of the observation group was remarkably lower than that of the control group (P<0.05). Figure 8 shows the typical cross-sectional morphological images of coronary vessels of the mice in the two groups. After comparing the cross-sectional morphology of normal blood vessels, the morphology of blood vessels in the observation group was much more similar to normal blood vessels compared with the control group.

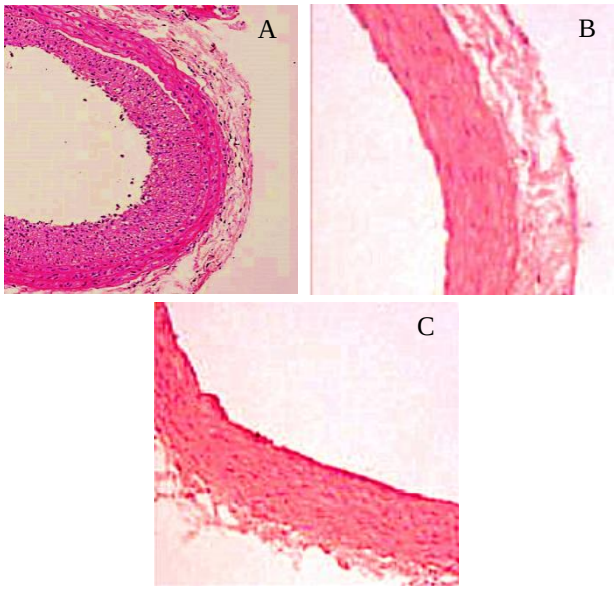

Figure 6. The observation results of OM (×200).

With the continuous development of China's industrialization and the increasing contact with western countries, people's living habits and diet have been greatly affected, which leads to an increased incidence of CAD in China. It has even become a fatal disease more harmful than cancer (18). In the course of CAD treatment, the prevention of coronary artery restenosis is a big problem. It has been proposed that PTX helps reduce the reconstruction of the restenosis and the blood supply at the lesion of vascular disease (19). However, when the vascular endothelium is damaged during surgery, the adoption of PTX isn't conducive to the healing of the endothelial tissue. The

transduction of the VEGF signal can affect the generation of blood vessels and promote the healing of vascular endothelial injury (20). Hence, in this experiment, a double-layer nanoparticle with VEGF as the shell and PTX as the kernel was established, which was applied in the surgical treatment of CAD patients by balloon perfusion.

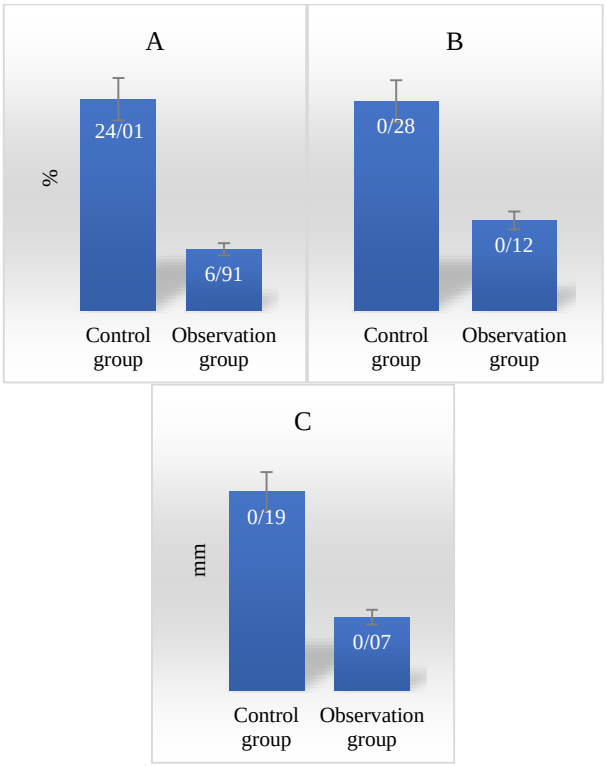

Figure 7. Comparison of restenosis. (A: restenosis; B: proliferation index; C: maximum intima thickness).

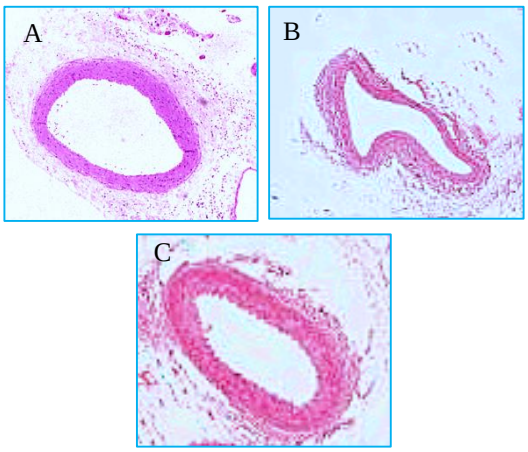

Figure 8. Cross-sectional morphology of coronary vessels.

The complete healing degree of vascular endothelium in the observation group was signally better than that in the control group under the OCT, which was consistent with the results of OM. It demonstrated that VEGF delivered by V-P-NPS could promote not only the proliferation of vascular endothelial tissue but also accelerate the healing of vascular endothelial tissue, which was consistent with the conclusion made by Amoli et al. (2012) (21). Furthermore, the double-layer nanoparticle could prevent the repair and inhibition of endothelial tissue by PTX. Zhang et al. (2021) (22) proposed that the double-layer nanoparticle was a hot topic of current research. Xia et al. (2020) (23) found that double-layer nanoparticle was conducive to controlling the action sequence of combined drugs, facilitating one-time treatment of diseases, or alleviating the effects of adverse drugs, with an ideal adoption value. Moreover, through this experiment, the restenosis of the observation group (stenosis (6.91±7.59) %), the proliferation index (0.12±0.02), and the maximum intima thickness (0.07±0.09) mm) were obviously decreased compared with the control group ((24.01±12.78) %, (0.28±0.01), (0.19±0.08) mm) (P<0.05). It indicated that V-P-NPS had a certain inhibitory effect on the occurrence of restenosis after the surgery of CAD, and the promotion of vascular endothelial healing by VEGF was of great significance for the prevention of restenosis. It was consistent with the conclusions of Chang et al. (2018) (24). Bagyura et al. (2017) (25) also proposed that VEGF could promote the proliferation of vascular smooth muscle cells, which supported the results of this work.

Firstly, the characterization of nanoparticles was analyzed, and the particle sizes of PTX-PNs and V-P-NPs were (270.29±1.89) nm and (251.12±1.19) nm, respectively. Particles with the size of 120-300nm are relatively easy to penetrate into the inner layer of blood vessels, which has been proposed in other research (26). The sizes of PTX-NPs and V-P-NPs prepared were within this range, so they could be used in the experiment. The size, distribution, and Zeta-potential of PTX-NPs and V-P-NPs had no considerable differences, which demonstrated that PTX-NPs had certain research feasibility. According to the results of the TEM of PTX-PNs and V-P-NPs, the dispersity of nanoparticles was good. The dispersity of nanoparticles in liquids was very important (27), and the nanoparticles prepared in this experiment had good dispersity, which met the requirements. The structures of the inner and outer

layers of V-P-NPs were obvious, which indicated that the preparation of the double-layer nanoparticle was successful. The entrapment efficiency of PTX in PTX-NPs and PTX and VEGF in V-P-NPs were 94.32%, 95.66%, and 97.89%, respectively, all of which were quite high. Oh et al. (2022) (28) proposed that high drug loading capacity and stable encapsulation were conducive to exerting the drug effects. The drug-loading rate of PTX-NPs and V-P-NPs were 28.91%, 30.12%, and 29.91%, respectively. There was no considerable difference between entrapment efficiency and drug-loading rate (P>0.05), with certain stability. In summary, the PTX-NPs and V-P-NPs used in this experiment had a good adoption effect, and the research results were reliable.

Conclusions

The animal model of CAD was established and treated by the double-layer nano-infusion technique. The development and changes of atherosclerosis and restenosis after local injection were assessed. The results reflected that the infusion therapy of double-layer nanoparticles was beneficial to the healing of vascular endothelial tissue, and it could inhibit vascular restenosis with a certain clinical adoption value. Nevertheless, this study isn't a clinical practice study, and further clinical research is needed to determine whether it can be effectively applied to clinical practice. Nonetheless, to a certain extent, this study provided support for subsequent clinical studies, and it also shows a good adoption prospect of the infusion of the double-layer nanoparticles.

Acknowledgments

Not applicable.

Interest conflict

The authors declare that they have no conflict of interest.

References

1. Papadiochou S, Pissiotis AL. Marginal adaptation and CAD-CAM technology: A systematic review of restorative material and fabrication techniques. J Prosthet Dent, 2018; 119(4): 545-551.
2. Lee UW, Ahn S, Shin YS, et al. Comparison of the CAD consortium and updated Diamond-Forrester scores for predicting obstructive coronary artery disease. Am J Emerg Med 2021; 43:200-204.
3. Charavet C, Van Hede D, Maes N, Albert A, Lambert F. Disentangling the effects of CAD/CAM customized appliances and piezocision in orthodontic treatment. Angle Orthod 2021; 91(6):764-771.
4. Aranki SF, Cohn LH. Comparing today's revascularization strategies for CAD. Benefits and drawbacks of thrombolytics, PTCA, CABG. J Crit Illn, 1995;10(8):523-534.
5. Wang Y, Zhan J, Bian W, Tang X, Zeng M. Local hemodynamic analysis after coronary stent implantation based on Euler-Lagrange method. J Biol Phys 2021;47(2):143-170.
6. Yang X, Yang Y, Guo J, et al. Targeting the epigenome in in-stent restenosis: from mechanisms to therapy. Mol Ther Nucleic Acids 2021; 23:1136-1160.
7. Feng S, Gao L, Zhang D, et al. MiR-93 regulates vascular smooth muscle cell proliferation, and neointimal formation through targeting Mfn2. Int J Biol Sci, 2019;15(12):2615-2626.
8. Anantha-Narayanan M, Love K, Nagpal S, Sheikh AB, Regan CJ, Mena-Hurtado C. Safety and efficacy of paclitaxel drug-coated balloon in femoropopliteal in-stent restenosis. Expert Rev Med Devices 2020;17(6):533-539.
9. Doggrell SA. Sirolimus- or paclitaxel-eluting stents to prevent coronary artery restenosis. Expert Opin Pharmacother 2004; 5(11): 2209-2220.
10. Wu R, Li Z, Wang M, Chang G, Yao C, Wang S. Paclitaxel-coated versus uncoated balloon angioplasty for femoropopliteal artery in-stent restenosis. Int J Surg 2017;42:72-82.
11. Katsaros KM, Kastl SP, Krychtiuk KA, et al. An increase of VEGF plasma levels is associated with restenosis of drug-eluting stents. EuroIntervention 2014;10(2): 224-230.
12. Lv YX, Zhong S, Tang H, et al. VEGF-A and VEGF-B Coordinate the Arteriogenesis to Repair the Infarcted Heart with Vagus Nerve Stimulation. Cell Physiol Biochem 2018;48(2): 433-449.
13. Song Y, Tang C, Yin C. Combination antitumor immunotherapy with VEGF and PIGF siRNA via systemic delivery of multi-functionalized nanoparticles to tumor-associated macrophages and breast cancer cells. Biomaterials 2018;185: 117-132.
14. Lee YW, Hwang YE, Lee JY, Sohn JH, Sung BH, Kim SC. VEGF siRNA Delivery by a Cancer-Specific Cell-Penetrating Peptide. J Microbiol Biotechnol 2018;28(3): 367-374.
15. Wang S, Guo H, Li Y, Li X. Penetration of nanoparticles across a lipid bilayer: effects of particle stiffness and surface hydrophobicity. Nanoscale 2019;11(9): 4025-4034.
16. Chan AS, Chen CH, Huang CM, Hsieh MF. Regulation of particle morphology of pH-dependent poly(epsilon-caprolactone)-poly(gamma-glutamic acid) micellar nanoparticles to combat breast cancer cells. J Nanosci Nanotechnol 2010;10(10): 6283-6297.
17. Bausback Y, Wittig T, Schmidt A, et al. Drug-Eluting Stent Versus Drug-Coated Balloon Revascularization in Patients With Femoropopliteal Arterial Disease. J Am Coll Cardiol 2019; 73(6): 667-679.

18. Kapos T, Evans C. CAD/CAM technology for implant abutments, crowns, and superstructures. Int J Oral Maxillofac Implants 2014; 29 Suppl 117-136.
19. Liistro F, Angioli P, Reccia MR, et al. Long-term mortality in patients undergoing lower-limb revascularization with Paclitaxel eluting devices. Int J Cardiol 2021; 339:150-157.
20. Ouyang S, Li Y, Wu X, et al. GPR4 signaling is essential for the promotion of acid-mediated angiogenic capacity of endothelial progenitor cells by activating STAT3/VEGFA pathway in patients with coronary artery disease. Stem Cell Res Ther 2021; 12(1): 149.
21. Amoli MM, Amiri P, Alborzi A, Larijani B, Saba S, Tavakkoly-Bazzaz J. VEGF gene mRNA expression in patients with coronary artery disease. Mol Biol Rep 2012; 39(9): 8595-8599.
22. Zhang Z, Ma W, He K, Yuan B, Yang K . Ligand-decoration determines the translational and rotational dynamics of nanoparticles on a lipid bilayer membrane. Phys Chem Chem Phys 2021; 23(15):9158-9165.
23. Xia Z, Lau BLT. Mitigating effects of osmolytes on the interactions between nanoparticles and supported lipid bilayer. J Colloid Interface Sci 2020; 568: 1-7.
24. Chang HK, Kim PH, Kim DW, et al. Coronary stents with inducible VEGF/HGF-secreting UCB-MSCs reduced restenosis and increased re-endothelialization in a swine model. Exp Mol Med 2018; 50(9):1-14.
25. agyura Z, Kiss L, Hirschberg K, et al. Association between VEGF Gene Polymorphisms and In-Stent Restenosis after Coronary Intervention Treated with Bare Metal Stent. Dis Markers 2017; 2017, pp. 9548612.
26. Villamil Giraldo AM, Kasson PM. Bilayer-Coated Nanoparticles Reveal How Influenza Viral Entry Depends on Membrane Deformability but Not Curvature. J Phys Chem Lett 2020; 11(17): 7190-7196.
27. Ilett M, Wills J, Rees P, et al. Application of automated electron microscopy imaging and machine learning to characterise and quantify nanoparticle dispersion in aqueous media. J Microsc, 2020; 279(3):177-184.
28. Oh JY, Yang G, Choi E, Ryu JH. Mesoporous silica nanoparticle-supported nanocarriers with enhanced drug loading, encapsulation stability, and targeting efficiency. Biomater Sci 2022; 10(6): 1448-1455.